GeV-TeV γ-ray light curves expected in the IC e$^\pm$ pair cascade model for massive binaries: application to LS 5039

W. Bednarek

Department of Experimental Physics, University of Łódź, 90-236 Łódź, ul. Pomorska 149/153, Poland
e-mail: bednar@fizwe4.fic.uni.lodz.pl

ABSTRACT

Context. TeV gamma-ray emission from two massive binaries of the microquasar type, LS 5039 and LS I +61° 303, show clear variability with their orbital periods.
Aims. Our purpose is to calculate the GeV and TeV γ-ray light curves from the massive binary LS 5039, which are expected in the specific inverse Compton e$^\pm$ pair cascade model. This model has successfully predicted the basic features of the high energy γ-ray emission from LS 5039 and LS I +61° 303.
Methods. In the calculations we apply the Monte Carlo code, which follows the IC e$^\pm$ pair cascade in the anisotropic radiation of the massive star.
Results. The γ-ray light curves and spectra are obtained for different parameters of the acceleration scenario and the inclination angles of the binary system. We find that the GeV and TeV γ-ray light curves should be anti-correlated. This feature can be tested in the near future by the simultaneous observations of LS 5039 with the AGILE and GLAST telescopes in GeV energies and the Cherenkov telescopes in the TeV energies. This model also predicts a broad maximum in the TeV γ-ray light curve between the phases ~0.4–0.8 consistently with the observations of LS 5039 by the HESS telescopes. Moreover, we predict an additional dip in the TeV light curve for large inclination angles ~60°. This feature could serve as a diagnostic for independently measuring the inclination angle of this binary system indicating also the presence of a neutron star in LS 5039.

Key words. gamma rays: theory – radiation mechanisms: non-thermal – binaries: close – stars: individual: LS 5039

1. Introduction

Recently, two massive binary systems of the microquasar type were discovered as TeV γ-ray sources, LS 5039 (Aharonian et al. 2005) and LS I +61° 303 (Albert et al. 2006). The TeV γ-ray emission is modulated with the orbital periods of these two binary systems (Albert et al. 2006; Aharonian et al. 2006a). This feature strongly indicates that high-energy processes already occur inside the binary systems not far from the massive star. In fact, this modulation of the γ-ray signals from these two binaries (the phases of the maximum emission) was recently predicted based on the calculations of the propagation of high-energy γ-rays inside massive binaries (Bednarek 2006a). The optical depths for TeV γ-rays inside these specific binary systems have also been calculated in other papers (e.g. Bötcher & Dermer 2005; Dubus 2006).

In this paper we concentrate on applying the detailed inverse Compton (IC) e$^\pm$ pair cascade model for the binary system LS 5039 (applied already to LS I +61° 303, Bednarek 2006b, B06). It is usually expected that this TeV γ-ray emission can appear in LS 5039 as a result of the comptonization of the stellar radiation by relativistic leptons in the jet (e.g. Paredes et al. 2006; Dermer & Böttcher 2006), although hadronic production of γ-rays has also been considered (e.g. Aharonian et al. 2006b; Romero et al. 2005). In our model, we take into account the effects of anisotropic cascade initiated by leptons in the radiation of the massive star including the synchrotron losses. We calculate the γ-ray light curves and spectra in the GeV and TeV

energy ranges and discuss them in the context of recently observed γ-ray light curve from LS 5039 (Aharonian et al. 2006a).

The basic parameters of the binary system LS 5039 were recently reported by Casares et al. (2005); the semi-major axis $a = 3.4\ r_\star$; ellipticity $e = 0.35 \pm 0.04$; the inclination of the binary system toward the observer, $i = 24.9 \pm 2.8^\circ$ for the case of the black hole with the mass 3.7 $M_\odot$ and ~60° for the neutron star; the azimuthal angle of the observer in respect to the periastron passage, $\omega = 225^\circ$; radius of the massive star, $r_\star = 9.3^{+0.7}_{-0.6}\ R_\odot$; and its surface temperature, $T_s = 3.9 \times 10^4$ K. For these parameters the distance of the compact object from the massive star is found in the range $r_p = 2.2\ r_\star$ at the periastron up to $r_a = 4.5\ r_\star$ at the apastron.

The binary system LS 5039 shows relativistic radio jets on miliarcsecond scales with the speed of ~0.3c (Paredes et al. 2000). It has been identified as a counterpart to the EGRET source 3EG J1824-1514, which has a relatively flat spectrum above 100 MeV with the spectral index <2 (Paredes et al. 2005). Moreover, the position of LS 5039 is consistent at the 3σ level with the recently detected TeV source HESS J1826-148 (Aharonian et al. 2005). The spectrum of this source above 250 GeV is also flat with the photon index 2.12 $\pm$ 0.15, although the flux is about two orders of magnitude lower than at GeV energies. Recent re-analysis of the TeV γ-ray light curve by Casares et al. (2005), using new orbital parameters, has shown possible flux variations of a factor ~3 with the maximum around the phase ~0.9. In fact, the HESS collaboration (Aharonian et al. 2006a) recently detected γ-ray emission from
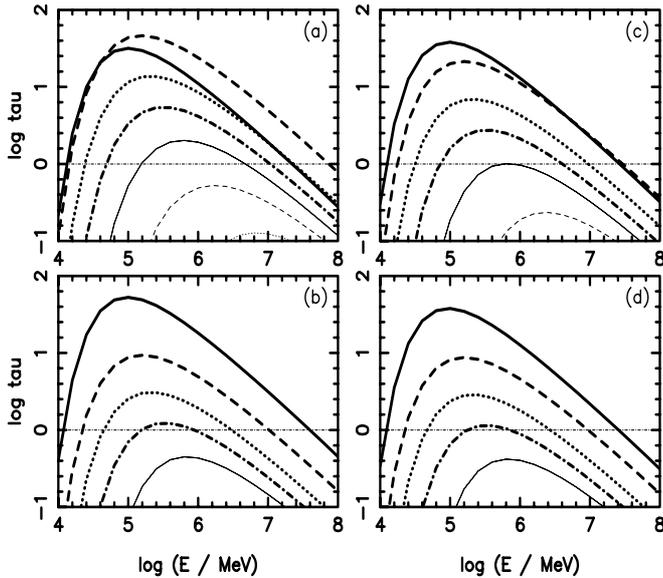
Fig. 1. The optical depths for γ-rays (as a function of their energy) on the $e^{\pm}$ pair production in collisions with stellar photons. γ-rays are injected in the jet at the distance from its base $z = 1r_{\star}$ (**a**) and **c**)) and $10r_{\star}$ (**b**) and **d**)) for the periastron passage (2.2 $r_{\star}$, left figures) and the apastron passage (4.5 $r_{\star}$, right figures) of the compact object on its orbit around the massive star in LS 5039. Specific curves show the optical depths up to infinity (except for the case in which photons only propagate to the stellar surface) for the injection angles of γ-rays, α, measured from the direction defined by the centers of the stars, $\alpha = 0^{\circ}$ (thick full curve, direction toward the massive star), 30° (thick dashed), 60° (thick dotted), 90° (thick dot-dashed), 120° (thin full), 150° (thin dashed), 180° (thin dotted).

this source that is clearly modulated with the orbital period of the binary system with possibly two peaks at the phases ~0.5–0.6 and ~0.8–0.9.

2. A microquasar in the compact massive binary

Details of the IC $e^{\pm}$ pair cascade model, which we want to apply to LS 5039, were recently described in Bednarek (B06, applied to another binary system LS I +61° 303). We call only the most important features of the model, concentrating on the issues that might be characteristic of LS 5039.

Leptons injected into the radiation field of the massive star initiate the IC $e^{\pm}$ pair cascade provided that, at least in some directions, the optical depths for γ-rays (in $\gamma + \gamma \rightarrow e^+e^-$ process) are above unity. We calculate these optical depths in the general case, i.e. for an arbitrary place of injection of γ-ray photons with arbitrary energies and angles of propagation, by applying the parameters of the massive star in LS 5039 (see Fig. 1). For a range of photon energies and their injection angles, the optical depths are clearly above unity. Thus, the basic conditions for applying such a model are fulfilled since the electrons in the jet tend to produce the first generation γ-rays in direction of the greatest optical depth.

We consider a simple geometrical scenario in which a two-sided jet is launched along the disk axis. For simplicity, we assume that the surface of the disk is in the plane of the binary system; i.e. the jet direction is perpendicular to the plane of the binary system. Relativistic leptons are injected along the jet at some range of distances from its base, starting at z_{min} up to z_{max}. The magnetic field strength, which determines the process of the acceleration of leptons in the jet and their losses in the
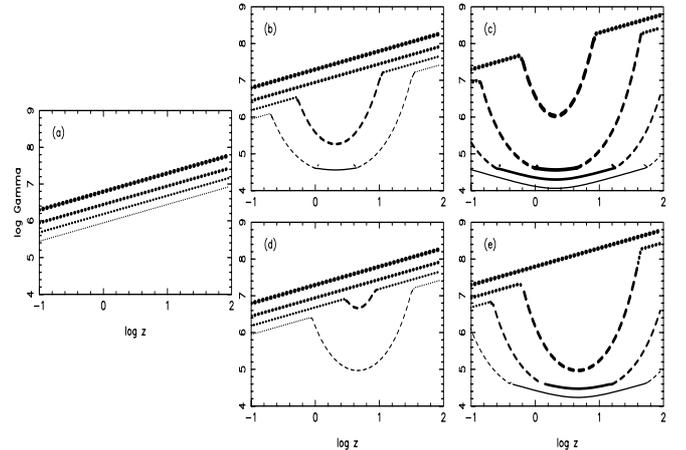

Fig. 2. The maximum Lorentz factors of electrons as a function of the distance, z, from the base of the jet (measured in units of the stellar radius) for different acceleration efficiencies: $\xi = 0.5$ (from the upper, thickest curve), 0.1, 0.03, and 0.001 (to the bottom, thinner curve) and the parameter describing the magnetic field at the base of the jet (at the inner radius of the accretion disk) equal to $B = 3 \times 10^5$ G **a**) ($\eta = 1$ – the equipartition of magnetic field with disk radiation), $\eta = 0.1$ (**b**) and **d**)), and 0.01 (**c**) and **e**)). The Maximum Lorentz factors are obtained from the comparison of the acceleration rate with the energy loss rate on synchrotron process (dotted lines), inverse Compton process in the Thomson regime (full curve) and the Klein-Nishina regime (dashed curves), for the periastron (**a**), **b**), and **c**)) and the apastron (**a**), **d**), and **e**)) passages of the compact object.

synchrotron process, is described by parameter η (the ratio of the magnetic field energy density to radiation energy density in the inner part of the accretion disk, see details of the model for the magnetic field in the jet in Bednarek (B06)). The energy losses of leptons in IC scattering in the Thomson and the Klein-Nishina regime are important as well. They are taken into account when considering the acceleration of electrons. We assume that leptons are accelerated with a power-law spectrum (and spectral index which does not depend on z) in multiple shocks propagating along the jet. The maximum energies of electrons are determined by the acceleration mechanism (defined by the acceleration parameter ξ) and by the energy losses on the most efficient radiation process (see B06). These maximum energies are shown for specific values of ξ and η as a function of the distance, z, from the base of the jet (Fig. 2). It is clear that, for reasonable values, leptons can reach energies over a few tens of TeV, already at distances from the base of the jet closer than 10 radii of the massive star.

We consider two different scenarios for the injection rate of relativistic leptons along the jet. This rate (electrons per unit length along the jet per unit time) is constant along the jet from its base at z_{min} up to z_{max} (i.e. $N(z) \propto$ const.), or it drops along the jet proportionally to the magnetic energy density in the jet starting from some distance, z_{min}, from the base of the jet (i.e. $N(z) \propto z^{-2}$).

3. The cascade γ-ray spectra

Since leptons are injected isotropically in the jet, they prefer to produce γ-rays in directions where they find the greatest optical depth. Therefore, absorption of γ-rays and interaction of secondary $e^{\pm}$ pairs have to be taken into account when calculating the γ-ray spectra produced by leptons in the radiation field of the massive star at both the periastron and the apastron passages.
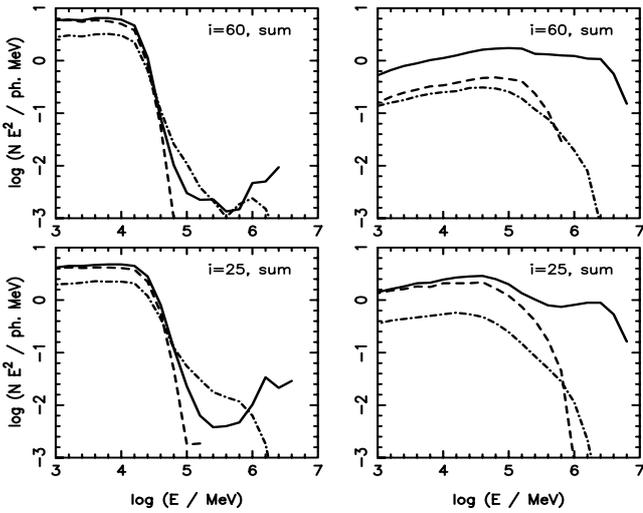
Fig. 3. Spectral Energy Distributions (SED) from cascades initiated by primary electrons injected in the jet with: the efficiency of electron injection depending on the distance from the base of the jet as $N(z) \propto z^{-2}$ (independently on the phase of the binary system), and differential power law spectrum of electrons with the index equal to -2. The left figures show the γ-ray spectra, produced at the periastron passage of the compact object for the observer located at the inclination angles $i = 25^{\circ}$ and 60°, from the *jet* and *counter-jet* (the *sum* of both). The jets propagate perpendicular to the plane of the binary system. The γ-ray spectra produced at the apastron passage of the compact object are shown on the right figures. The specific spectra are calculated for the acceleration conditions in the jet described by the parameters: $\xi = 0.03$ and $\eta = 0.1$ (full curves), $\xi = 0.3$ and $\eta = 0.01$, (dashed), and $\xi = 0.3$ and $\eta = 0.1$ (dot-dashed).

We performed the Monte Carlo calculations of the γ-ray spectra escaping from the binary system at arbitrary directions, applying the above-mentioned model for the acceleration of primary leptons in the jet. To allow a simple analysis, at first we considered the case of injection of leptons in the jet with the power-law spectrum and a differential spectral index equal to -2, with the cut-off that depends on the location of the acceleration place in the jet and on the phase of the compact object (see Fig. 2). These cut-offs are determined by the values of η and ξ. Since two jets are expected from a single compact object, we considered the production of γ-rays in the jet that propagate above the plain of the binary system (i.e. the *jet* directed towards the hemisphere containing the observer) and in the jet propagating below the plane of the binary system (i.e. the *counter-jet*); see (B06).

The results of example calculations of the γ-ray spectra from the IC $e^{\pm}$ pair cascade are shown in Fig. 3 for different values of ξ and η. The observer is located at the inclination angles of 25° and 60°. The spectra are shown for the compact object at the periastron (left figures) and the apastron passages (right). The γ-ray spectra, produced by leptons injected in the jet at the periastron passage, steepen significantly at energies above a few tens of GeV due to the efficient cascading. These cascading effects are significantly smaller when the compact object is close to the apastron. However, note that the γ-ray spectra calculated for these parameters do not fit nicely to the spectra observed recently by Aharonian et al. (2006a) due to the deficit in γ-ray emission above $\sim$100 GeV. Therefore, in the next section we consider the model with the flatter profile for the injection of electrons into the jet (i.e. $N(z) = $ const.).
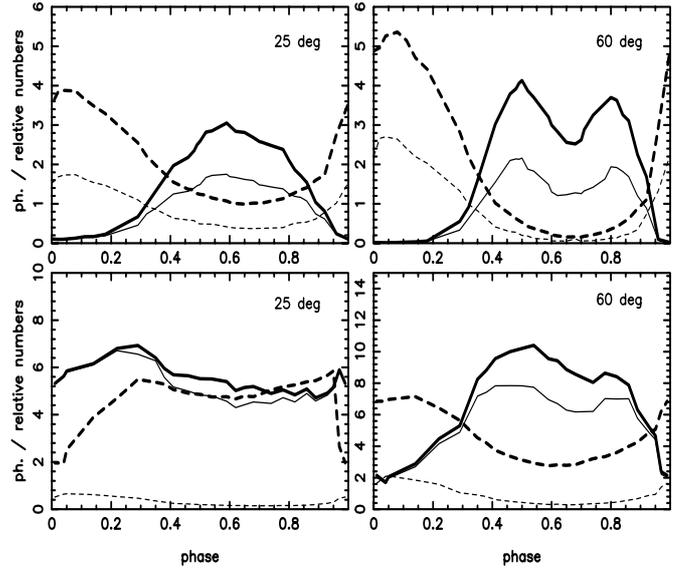

Fig. 4. The γ-ray light curves in the energy range 1–10 GeV (dashed curves) and >300 GeV (full curves), produced by electrons in the jet (thin curves) and the jet + counter-jet (thick curves), are shown on the upper panel for two possible inclination angles of the binary system LS 5039 (25° and 60°), $\xi = 0.1$, $\eta = 0.1$, $z_{\min} = 0.1 \, r_{\star}$, and $z_{\max} = 10 \, r_{\star}$. On the bottom panel, the γ-ray light curves are shown for $\xi = 0.2$, $\eta = 0.1$, and $z_{\max} = 20 \, r_{\star}$.

4. Confrontation with observations of LS 5039

Let us select the set of parameters that allows acceleration of electrons to energies up to $\sim$10 TeV (see upper panels in Fig. 2). For these parameters ($\xi = 0.1$ and $\eta = 0.1$) and the case of electrons injected with the constant rate along the jet between $z_{\min} = 0.1 \, r_{\star}$ and $z_{\max} = 10 \, r_{\star}$, we calculate the γ-ray light curves in two energy ranges, i.e. 1–10 GeV (the GeV region, the AGILE and GLAST energy range) and >300 GeV (the TeV region, the Cherenkov telescopes energy range), and two possible inclination angles of the binary system LS 5039, i.e. 25° and 60° (the range of angles derived by Casares et al. 2005). The TeV γ-ray light curves, calculated for 25°, show a broad maximum between the phases $\sim$0.4–0.8 peaked at the phase $\sim$0.6. On the other hand, the light curves for the inclination angle 60° show a more complicated structure. The broad maximum between the phases $\sim$0.4–0.8 clearly shows two additional peaks centered at the phases $\sim$0.5 and $\sim$0.8 and a dip at the phase $\sim$0.65 (Fig. 4). The general broad maximum observed for both inclination angles is consistent with recently reported TeV γ-ray light curve observed by the HESS collaboration (see the bottom panel in Fig. 5 in Aharonian et al. 2006a). Note, however that the HESS TeV γ-ray light curve also shows – although not statistically very significant – a dip in the maximum at the phase $\sim$ 0.65, corresponding to the interior conjunction of the compact object. The confirmation of such a structure by the future HESS observations will strongly argue for the inclination of the binary system closer to 60°, supporting the hypothesis of the presence of a neutron star in this binary system.

Note that Böttcher (2006) argues for an inclination angle of the LS 5039 closer to 30°, based on the de-absorption of the γ-ray spectrum observed by the HESS experiment from LS 5039. However, these calculations based on the assumption that the cascading processes initiated by secondary leptons (originated in the absorption process of TeV γ-rays) in the radiation of the massive star, can be neglected. This is valid, provided that the

magnetic field inside the volume of the binary system is strong enough to guarantee efficient cooling of secondary pairs in synchrotron process (in the case of LS 5039 should be of the order of ~100 G). In another case discussed in this paper, the IC $e^\pm$ pair cascades should be taken into account since the cross sections for γ–γ absorption and IC scattering in the KN regime are similar; see e.g. the optical depths for these two processes in Fig. 2 in Sierpowska & Bednarek (2005).

In our model the broad maximum between phases ~0.4–0.8 in the TeV γ-ray light curve is due to the favorite location of the compact object in respect to the massive star and the observer. At these phases, the jet is generally on the other side of the massive star with respect to the observer, and the conditions for scattering of stellar radiation by electrons in the jet into the TeV γ-ray energy range are optimal. However, when the line of sight to the compact object passes very close to the massive star, which occurs in the case of large inclination angles, absorption of TeV γ-rays in the stellar radiation starts to play a dominant role. This is the reason for the appearance of additional dip in the TeV light curve at phase ~0.65 for large inclination angles of the binary system. For low inclination angles, the line of sight is sufficiently distant from the massive star, and the absorption effects of TeV γ-rays are too low to produce additional dip in the light curve.

On the other hand, the GeV γ-ray light curve behaves very differently. It is clearly anti-correlated with the TeV γ-ray emission. This is caused by more efficient cascading close to the periastron passage of the compact object in which many GeV photons are created. In directions where the optical depths of TeV γ-rays are large, the energy from electrons, originally transferred to primary TeV γ-rays, is degraded to the GeV γ-rays. In contrast, TeV γ-rays in directions of low optical depths, escape with relatively mild absorption, thereby producing the peak in the TeV light curve. Therefore, the maximum in the GeV γ-ray light curve appears just after periastron, at the phase ~0.05 (i.e. at the superior conjunction of the compact object), and the minimum at the phase ~0.7 (i.e. at the inferior conjunction). It is expected that the GeV γ-ray emission may vary by a factor up to ~30 with the period of LS 5039 (see Fig. 4). Hence, we also predict strong modulation of the GeV emission from LS 5039 with its orbital period, which should be easily observed by the AGILE and GLAST detectors.

Note that the TeV γ-ray light curve, reported by Aharonian et al. (2006a, Fig. 5), also shows clear base line emission at the periastron passage of the compact object. In order to check if this emission can originate farther along the jet, we show in the bottom panel in Fig. 4 the γ-ray light curves for the case of injection of electrons in the jet up to $z_{max} = 20\ r_\star$, $\xi = 0.2$, and $\eta = 0.1$. In fact, this base-line emission at a level of ~20% of the

peak emission appears close to the periastron for the inclination angle $i = 60^\circ$. Moreover, previously found two peak structure is still present in the TeV γ-ray light curve (or broad high level emission through the phases ~0.4–0.8) for the case of inclination angle of the binary system $i = 60^\circ$. However, in contrast to the previously discussed case in the upper panels in Fig. 4, the TeV γ-ray light curve for the inclination angle 25° is quite flat due to similar conditions farther along the jet, independent of the periastron or apastron location of the compact object.

The spectral features observed by the HESS (Aharonian et al. 2006a), i.e. a flat power spectrum at the inferior conjunction and steep spectrum at the superior conjunction, can also be explained in terms of the present general model. These features even appear in such a simplified model for the injection of relativistic electrons in the jet (see Fig. 3), i.e single power-law spectra for the electrons and their injection rate independent of the phase of the compact object. Based on these results, we conclude that a more realistic model (which relax these simple assumptions) can certainly produce exact fitting of the experimental spectral data, although huge computation-time requirements prevent this sort of direct comparison at present. Since in our model the cooling of electrons in the jet of the IC process is very efficient (Bednarek 2006b) and the injection rate of electrons does not depend on the phase of the compact object, the total requirement on the energy budget of accelerated electrons is comparable to the power emitted in the γ-rays in the high state, i.e. close to the inferior conjunction.

References

Aharonian, F., Akhperjanian, A. G., Aye, K. M., et al. (HESS collab.) 2005, Science, 309, 746
Aharonian, F., Akhperjanian, A. G., Aye, K. M., et al. (HESS collab.) 2006a, A&A, 460, 743
Aharonian, F., Anchordoqui, L., Khangulyan, D., & Montaruli, T. 2006b, J. Phys. Conf. Ser., 39, 408
Albert, J., Aliu, E., Anderhub, H., et al. (MAGIC collab.) 2006, Science, 312, 1771
Bednarek, W. 2006a, MNRAS, 368, 579
Bednarek, W. 2006b, MNRAS, 371, 1737 (B06)
Böttcher, M. 2006, APh, in press [astro-ph/0609136]
Böttcher, M., & Dermer, C. D. 2005, ApJ, 634, L81
Casares, J., Ribo, M., Ribas, I., et al. 2005, MNRAS, 364, 899
Dermer, C.D., & Böttcher, M. 2006, ApJ, 643, 1081
Dubus, G. 2006, A&A, 451, 9
Paredes, J. M., Marti, J., Ribo, M., & Massi, M. 2000, Science, 288, 2340
Paredes, J. M., Bosch-Ramon, V., & Romero, G. E. 2006, A&A, 451, 259
Romero, G. E., Christiansen, H. R., & Orellana, M. 2005, ApJ, 632, 1093
Sierpowska, A., & Bednarek, W. 2005, MNRAS, 356, 711